


Conditional *Ror1* knockout reveals crucial involvement in lung adenocarcinoma development and identifies novel HIF-1 α regulator

Hisanori Isomura^{1,2} | Ayumu Taguchi^{2,3} | Taisuke Kajino^{1,2} | Naoya Asai^{4,5} | Masahiro Nakatochi⁶  | Seiichi Kato⁷ | Keiko Suzuki¹ | Kiyoshi Yanagisawa¹ | Motoshi Suzuki^{1,8}  | Teruaki Fujishita⁹ | Tomoya Yamaguchi^{1,10,11}  | Masahide Takahashi⁴ | Takashi Takahashi^{1,12} 

¹Division of Molecular Carcinogenesis, Center for Neurological Diseases and Cancer, Nagoya University Graduate School of Medicine, Nagoya, Japan

²Division of Molecular Diagnostics, Aichi Cancer Center Research Institute, Nagoya, Japan

³Division of Advanced Cancer Diagnostics, Department of Cancer Diagnostics and Therapeutics, Nagoya University Graduate School of Medicine, Nagoya, Japan

⁴Department of Pathology, Nagoya University Graduate School of Medicine, Nagoya, Japan

⁵Department of Pathology, Fujita Health University School of Medicine, Toyoake, Japan

⁶Public Health Informatics Unit, Department of Integrated Health Sciences, Nagoya University Graduate School of Medicine, Nagoya, Japan

⁷Department of Pathology and Molecular Diagnostics, Aichi Cancer Center Hospital, Nagoya, Japan

⁸Department of Molecular Oncology, Fujita Health University School of Medicine, Toyoake, Japan

⁹Division of Pathophysiology, Aichi Cancer Center Research Institute, Nagoya, Japan

¹⁰Department of Cancer Biology, Graduate School of Medical Sciences, Kumamoto University, Kumamoto, Japan

¹¹Center for Metabolic Regulation of Healthy Aging, Kumamoto University, Kumamoto, Japan

¹²Aichi Cancer Center, Nagoya, Japan

Correspondence

Takashi Takahashi, Aichi Cancer Center, 1-1 Kanokoden, Chikusa-ku, Nagoya 464-8681, Japan.
Email: tak@aichi-cc.jp

Funding information

the Japan Society for the Promotion of Science, Grant/Award Number: 16H02468; Japan Agency for Medical Research and Development, Grant/Award Number: JP18cm0106107 and JP20cm0106107

Abstract

We previously reported that *ROR1* is a crucial downstream gene for the *TTF-1/NKX2-1* lineage-survival oncogene in lung adenocarcinoma, while others have found altered expression of *ROR1* in multiple cancer types. Accumulated evidence therefore indicates *ROR1* as an attractive molecular target, though it has yet to be determined whether targeting *Ror1* can inhibit tumor development and growth in vivo. To this end, genetically engineered mice carrying homozygously floxed *Ror1* alleles and an SP-C promoter-driven human mutant *EGFR* transgene were generated. *Ror1* ablation resulted in marked retardation of tumor development and progression in association with reduced malignant characteristics and significantly better survival. Interestingly, gene set enrichment analysis identified a hypoxia-induced gene set (HALLMARK_HYPOXIA) as most significantly downregulated by *Ror1* ablation in vivo, which led to findings showing that *ROR1* knockdown diminished HIF-1 α expression under normoxia and clearly hampered HIF-1 α induction in response to hypoxia in human lung

This is an open access article under the terms of the Creative Commons Attribution-NonCommercial-NoDerivs License, which permits use and distribution in any medium, provided the original work is properly cited, the use is non-commercial and no modifications or adaptations are made.

© 2021 The Authors. Cancer Science published by John Wiley & Sons Australia, Ltd on behalf of Japanese Cancer Association.

adenocarcinoma cell lines. The present results directly demonstrate the importance of *Ror1* for in vivo development and progression of lung adenocarcinoma, and also identify *Ror1* as a novel regulator of Hif-1 α . Thus, a future study aimed at the development of a novel therapeutic targeting ROR1 for treatment of solid tumors such as seen in lung cancer, which are frequently accompanied with a hypoxic tumor micro-environment, is warranted.

KEYWORDS

EGFR, genetically engineered mouse model, HIF-1 α , lung adenocarcinoma, ROR1

1 | INTRODUCTION

Receptor tyrosine kinase-like orphan receptor 1 (ROR1) is an evolutionarily conserved type-I transmembrane receptor tyrosine kinase¹ that plays an essential role in embryonic development.^{2,3} Although ROR1 expression becomes markedly diminished after birth,^{4,5} accumulating evidence indicates that it is highly upregulated and involved in various malignancies, including those of the lung, breast, pancreas, skin, ovary, and colon, and also hematopoietic cells.⁴⁻¹² Four independent groups including our own have reported that the homeodomain transcription factor TTF-1/NKX2-1 plays a role as a lineage-survival oncogene in lung adenocarcinoma.¹³⁻¹⁶ However, that cannot be utilized as a molecular target for treatment, because of its essential roles for not only lung morphogenesis but also normal lung physiology, such as surfactant protein production and secretion.^{17,18} Along this line, our subsequent identification of ROR1 as a direct transcriptional target of TTF-1/NKX2-1 in lung adenocarcinoma makes this molecule an attractive potential molecular target for treatment of lung adenocarcinoma.⁶ ROR1 sustains EGFR-mediated PI3K-AKT pro-survival signaling and inhibits ASK1-p38 MAPK pro-apoptotic signaling in both kinase-dependent and kinase-independent manners,^{6,9} while it also maintains caveolae structure and caveolae-dependent endocytosis by functioning as a scaffold protein for caveolin-1, cavin-1, and cavin-3 in a kinase-independent fashion, and sustaining pro-survival signaling of other receptor tyrosine kinases (RTKs) including MET and IGF1R.^{7,8}

The present study was conducted to explore the importance of *Ror1* in tumor development in vivo using an animal model. To this end, genetically engineered mice carrying both homozygous floxed *Ror1* alleles and the SP-C promoter-driven human mutant *EGFR* transgene were generated, which enabled the investigation of the roles of *Ror1* in a lung adenocarcinoma model. The results are the first to show that *Ror1* ablation inhibits tumor development in mice and significantly increases the survival of those bearing mutant *EGFR*-elicited tumors. In addition, evidence indicating a novel function of ROR1 to sustain expression of HIF-1 α , a master transcriptional regulator of hypoxia-induced genes, is presented.

2 | MATERIALS AND METHODS

2.1 | Generation of mouse models

All animal studies were performed after receiving approval for the protocols from the Institutional Animal Care and Use Committee of Nagoya University Graduate School of Medicine and Aichi Cancer Center. In brief, a neo-loxP cassette carrying the FRT-flanked PGK promoter-driven Neo gene was inserted into intron 4 of the *Ror1* gene, while diphtheria toxin A-fragment (DT-A) driven by the PGK promoter was placed at the 5' of the targeting genomic fragment (Figure 1A). Mouse C57BL/6 ES cells were transfected with the targeting vector by electroporation, and G418-resistant clones were screened for homologous recombination by PCR. Positive clones were injected into Balb/c blastocysts to generate *Ror1*^{+/NeofRT} mice, which were crossed with *FLPe* transgenic mice to remove the Neo cassette. Offspring were backcrossed to wild-type C57BL/6J mice to remove the *CAG-FLPe* transgene, resulting in generation of *Ror1*^{+/ff} mice. Germline *Ror1* knockout mice were generated by crossing *Ror1*^{+/ff} and *CAG-Cre* mice, obtained from the Jackson Laboratory. *Ror1*^{+/ff} mice were also crossed with *CAG-CreER* transgenic mice from the Jackson Laboratory and the resultant *Ror1*^{+/ff}; *CAG-CreER* was used to conditionally ablate the endogenous *Ror1* gene upon induction of Cre recombinase in response to tamoxifen (TAM) administration.

To generate human mutant *EGFR* transgenic mice, a mutant *EGFR* construct lacking residues 746-750 was generated by introducing a deletion into the wild-type pcDNA3.1-EGFR vector using a KOD -Plus- Mutagenesis Kit (TOYOBO, SMK-101). The primers were F: 5'-ACATCTCCGAAAGCCAACAAG-3' and R: 5'-CTTGATAGCGACGGGAATTTT-3'. The full-length mutant *EGFR* cDNA and poly(A) addition signal sequence were amplified using the mutant pcDNA3.1-EGFR vector as a template using PCR primers containing a Sall site for cloning. The primers were F: 5'-AAAGTCGACATGCGACCCTCCGGGACGGC-3' and R: 5'-AAAGTCGACTCATGCTCCAATAAATTCAC-3'. After digestion with Sall, the amplified product was cloned downstream of the surfactant protein C (SP-C) promoter in the pUC18 vector (a generous gift from Prof. Jeffery Whitsett). This mutant *EGFR* expression cassette was excised by NotI digestion and injected into fertilized C57BL/6J eggs.

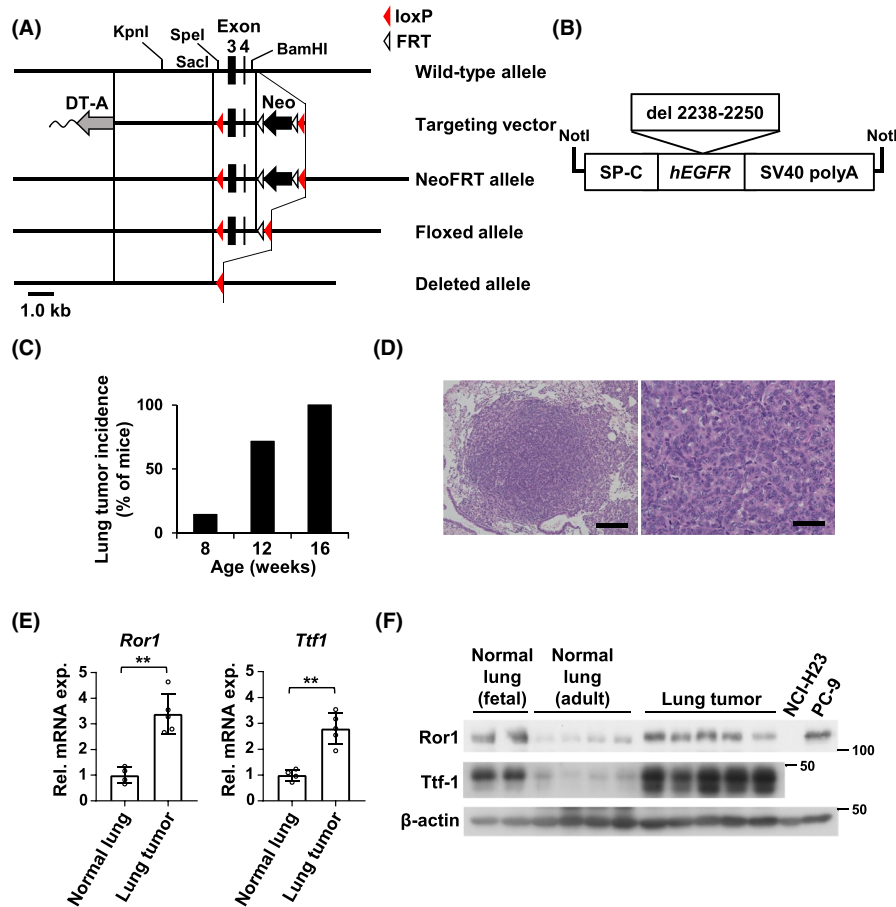


FIGURE 1 Generation of *Ror1^{f/f}*; *CAG-CreER*; *SPC-hEGFR^{del746-750}* (RCE) mice. **A**, Schematic of wild-type *Ror1* allele, targeting vector, and targeted NeofRT, floxed, and deleted allele. Recognition sites for KpnI, SacI, SpeI, and BamHI in the flanking region of exons 3 and 4 (filled boxes) are indicated. In the targeting vector, a 1.7-kb DNA fragment carrying exons 3 and 4 and its flanking region was replaced by a 3.5-kb fragment carrying 2 loxP sequences (red arrowheads) and PGK-neo (*Neo^R*) flanked by FRT sequences (open arrowheads). *Diphtheria toxin A*-fragment (DT-A; grey arrow) driven by the PGK promoter was inserted at 5' site of the vector. Scale bar represents 1.0 kb. **B**, Diagram of construct used to produce human mutant *EGFR* transgenic mice. **C**, Incidence of lung tumors in RCE mice determined by micro-CT observation. **D**, Representative H&E staining of lung tumors from RCE mice at 16 weeks of age. Scale bars represent 200 μ m (left) and 50 μ m (right). **E**, Expression of *Ror1* and *Ttf1* mRNA in lung tumors in *Ror1^{f/f}*; *SPC-hEGFR^{del746-750}* (RE) mice as well as in normal lung tissues of *Ror1^{f/f}* mice, both at 19 weeks of age. qRT-PCR analysis was performed using representative lung tumors and normal lung tissues, one each from five RE and four *Ror1^{f/f}* mice, respectively. Columns and bars indicate average and standard deviation, respectively. *P*-values were calculated using a two-tailed Student's *t*-test. ***P* < .01. **F**, Expression of *Ror1* and *Ttf-1* protein in lung tumors and normal lung tissues in RE and *Ror1^{f/f}* mice, respectively, at 19 weeks of age. Fetal lung tissues were obtained from *Ror1^{f/f}* mice on day E18.5. NCI-H23 and PC-9 cell lysates were used as negative and positive controls, respectively. β -actin served as a loading control

2.2 | Animal husbandry, genotyping, and treatment

All animals were maintained in specific pathogen-free housing with adequate food and water according to guidelines approved by the Nagoya University Graduate School of Medicine and Aichi Cancer Center. Genomic DNA samples from mouse tail snips or ear punch samples were used for PCR genotyping. The primer sequences for PCR genotyping are listed in Table S1. For conditional knockout of *Ror1*, mice were injected intraperitoneally with TAM (100 mg/kg body weight) once every 5 days from 8 to 30 weeks of age. Cre-mediated recombination of the floxed *Ror1* alleles by TAM administration was confirmed by PCR using the following primer pair: *Ror1* F: 5'-CTATCAATAAGAAGGTTTAGGG-3' and *Ror1* R:

5'-CTCTCCCTCCTCTTTGTGAG-3'. Gefitinib (10 mg/kg; SML1657, Sigma-Aldrich) or the vehicle was administered by oral gavage once daily for 4 days.

2.3 | Isolation of mouse embryonic fibroblasts (MEFs)

Mouse embryonic fibroblasts were prepared from day-13.5 embryos of *Ror1^{f/f}* and *Ror1^{f/f}*; *CAG-CreER* mice, as described in Supplementary Methods. MEFs after four passages were treated for 5 days with 4-hydroxytamoxifen (4-OHT) to ablate the *Ror1* floxed alleles, followed by harvesting for DNA and protein extraction.

2.4 | Micro-CT analysis

From 8 weeks of age, each mouse was anesthetized with isoflurane and scanned weekly using a SkyScan 1176 micro-CT analyzer. For acquisition of micro-CT images, 282 projection data were collected in one full rotation of the gantry at X-ray settings of 80 kV and 313 μ A with aluminum and copper filters. All images were reconstructed using the N-Recon program according to the manufacturer's protocol. Tumor volume in CT images was estimated by subtracting volume that exhibited air from total lung volume using Image J software (<https://imagej.nih.gov/ij/>). Normal pulmonary blood vessels were difficult to distinguish from similarly sized small tumors; thus they were included together with tumors in the calculation. Total tumor volume was calculated as the sum of tumors in two axial planes: one encompassing the seventh vertebra and the space between the third and fourth sternbrae, and the other the ninth vertebra and the space between the fourth and fifth sternbrae (Figure S1).

2.5 | Western blotting and quantitative real-time (qRT)-PCR analyses

Western blotting analyses were performed according to standard procedures using Immobilon-P filters (Millipore), an enhanced chemiluminescence system (GE Healthcare), and antibodies listed in Table S2. qRT-PCR analysis was also performed according to standard procedures, as described in Supplementary Methods, with the primers listed in Table S3. A TaqMan gene expression assay (Applied Biosystems) was also used to determine *Ror1* (Mm00443463_m1), *Ttf-1* (Mm00447558_m1), and *18s* (Hs99999901_s1) mRNA expression.

2.6 | Immunohistochemistry

Mouse tissues were collected, then fixed with 10% neutral buffered formalin for 48 hours at room temperature before embedding in paraffin. Hematoxylin and eosin (H&E) and immunohistochemical staining was performed using standard methods, as described in detail in Supplementary Methods. Two investigators (NA and HI) determined the percentage of MCM2-positive cells in 24 tumors from three TAM-treated mice and 27 tumors from three control mice under 10 \times magnification.

2.7 | Microarray analysis

To obtain gene expression data using a dye-swap strategy (GSE161182), 50 ng of total RNA from tumor tissues of TAM-treated ($n = 3$) and control ($n = 3$) *Ror1^{ff}*; *CAG-CreER*; *SPC-hEGFR^{del746-750}* mice was used for fluorescent (Cy-5 or Cy-3) generation of labeled cDNA. Microarray analysis was done using SurePrint G3 Mouse 8x60K Microarray G4851B, ver. 2 (Agilent Technologies) and GeneSpring,

ver. 13.1 (Agilent), essentially as previously described.¹⁹ Gene set enrichment analysis (GSEA) was performed²⁰ as detailed in Supplementary Methods.

2.8 | Cell cultures

NCI-H23 and NCI-H1975 cells were purchased from the American Type Culture Collection, and PC-9 cells from RIKEN Cell Bank. NCI-H1975 cells overexpressing siRNA-resistant wild-type (ROR1-WTm) or kinase-dead (ROR1-KDm) ROR1 used in the reconstitution experiments were previously reported.⁶ NCI-H1975 and PC-9 cells were free from mycoplasma contamination and authenticated by short tandem repeat DNA profiling performed in February 2019 at the Japanese Collection of Research Bioresources, National Institute of Biomedical Innovation of Japan. NCI-H1975 and PC-9 cells were grown under a normoxia (21% O₂) or hypoxia (1% O₂) condition for 24 hours at 37°C/5% CO₂ and then harvested for Western blotting and qRT-PCR analyses.

2.9 | siRNA and transfection

NCI-H1975 and PC-9 cells were transfected with 20 nmol/L siRNA using Lipofectamine RNAiMAX (Life Technologies), according to the manufacturer's instructions, using the following siRNAs: sicontrol (AllStars Negative Control siRNA, Qiagen) and siROR1 (Hs_ROR1_3, Qiagen). Cells were cultured for 24 hours and then placed under hypoxia or normoxia for 24 hours, with and without 5 μ mol/L MG132 or DMSO for the final 6 hours prior to harvesting.

2.10 | Statistical analysis

Continuous variables were compared using a two-tailed unpaired Student's *t*-test. Survival analysis was performed using Kaplan-Meier survival curves. A log-rank test was used to evaluate the statistical significance of differences of survival curves. Statistical analysis was done using the Prism 8.0 application (GraphPad).

3 | RESULTS

To determine the roles of *Ror1* in lung adenocarcinoma development in vivo in an animal model, we generated *Ror1* conditional knockout mice by placing *loxP* sites at the 5' and 3' positions of exons 3 and 4, respectively, of the *Ror1* gene (*Ror1^{ff}*; Figure 1A), in which all major functional domains were deleted upon Cre induction. To confirm the occurrence of intended loss of functional *Ror1* by recombination, germline *Ror1* knockout mice were first generated by crossing *Ror1^{ff}* with *CAG-Cre* transgenic mice. While *Ror1*-heterozygous mice did not exhibit any obvious phenotypes, intercrosses of *Ror1*-heterozygous mice resulted in neonatal lethality in germline homozygous *Ror1*

knockout mice (Figure S2A), a finding consistent with a previous study.² Next, *Ror1^{fl/fl}* mice were crossed with CAG-CreER transgenic mice, which made it possible to ablate the endogenous *Ror1* gene upon induction of Cre recombinase in response to TAM administration. To validate generation of *Ror1*-null alleles by recombination of the floxed *Ror1* alleles, MEFs isolated from E13.5 embryos of *Ror1^{fl/fl}* and *Ror1^{fl/fl}; CAG-CreER* mice were treated in vitro with 4-OHT for 5 days. We observed efficient recombination of the *Ror1* gene, leading to nearly complete depletion of *Ror1* expression in *Ror1^{fl/fl}; CAG-CreER* MEFs, but not in *Ror1^{fl/fl}* MEFs (Figure S2B,C).

The in vivo effects of *Ror1* depletion in adulthood were first investigated using conditional knockout mice. *Ror1^{fl/fl}; CAG-CreER* mice were injected intraperitoneally with TAM (100 mg/kg body weight) or oil once every 5 days from 8 to 30 weeks of age. While recombination of *Ror1* was confirmed in normal organs, including lung, stomach, small intestine, colon, liver, kidney, and spleen tissues (Figure S3A), all *Ror1^{fl/fl}; CAG-CreER* mice with TAM administration appeared healthy, and no significant differences in body weight or survival were observed between *Ror1^{fl/fl}; CAG-CreER* mice administered with TAM and those that received oil (data not shown). In addition, Western blot analysis showed a low but appreciable level of *Ror1* mRNA expression in mice without Cre induction (Figure S3B), whereas no appreciable pathologic changes were observed in the lung, stomach, small intestine, colon, liver,

kidney, or spleen tissues of *Ror1^{fl/fl}; CAG-CreER* mice with TAM administration (Figure S3C), suggesting that *Ror1* is not essential in adulthood.

A lung adenocarcinoma model was also established by generating transgenic mice expressing human mutant *EGFR* driven by the pulmonary SP-C promoter, which is active only in type II alveolar epithelial cells (*SPC-hEGFR^{del746-750}*; Figure 1B). Twenty-seven pups were obtained following injection of the transgene into fertilized eggs. A line positive for the transgene-produced offspring that developed lung adenocarcinoma at 8 weeks of age or older was then selected for further analysis. *Ror1^{fl/fl}; CAG-CreER* and *Ror1^{fl/fl}* mice were crossed with *SPC-hEGFR^{del746-750}* mice, which generated *Ror1^{fl/fl}; CAG-CreER; SPC-hEGFR^{del746-750}* (hereafter RCE) and *Ror1^{fl/fl}; SPC-hEGFR^{del746-750}* (hereafter RE) mice, respectively. qRT-PCR assays using human *EGFR*-specific primers and mRNAs extracted from various tissues confirmed lung-specific expression of human *EGFR* (Figure S4A). RCE mice developed multifocal lung adenocarcinomas at 8 weeks of age or older, with 100% incidence by 16 weeks of age, the same as observed in *SPC-hEGFR^{del746-750}* mice (Figure 1C,D). Treatment with gefitinib led to rapid tumor regression, suggesting that lung tumors driven by human mutant *EGFR* are highly dependent on *EGFR* signaling (Figure S4B,C). Furthermore, increased levels of expression of *Ror1* and *Ttf-1/Nkx2-1* at both the mRNA and protein levels were noted in the lung tumors as compared with normal lung tissues

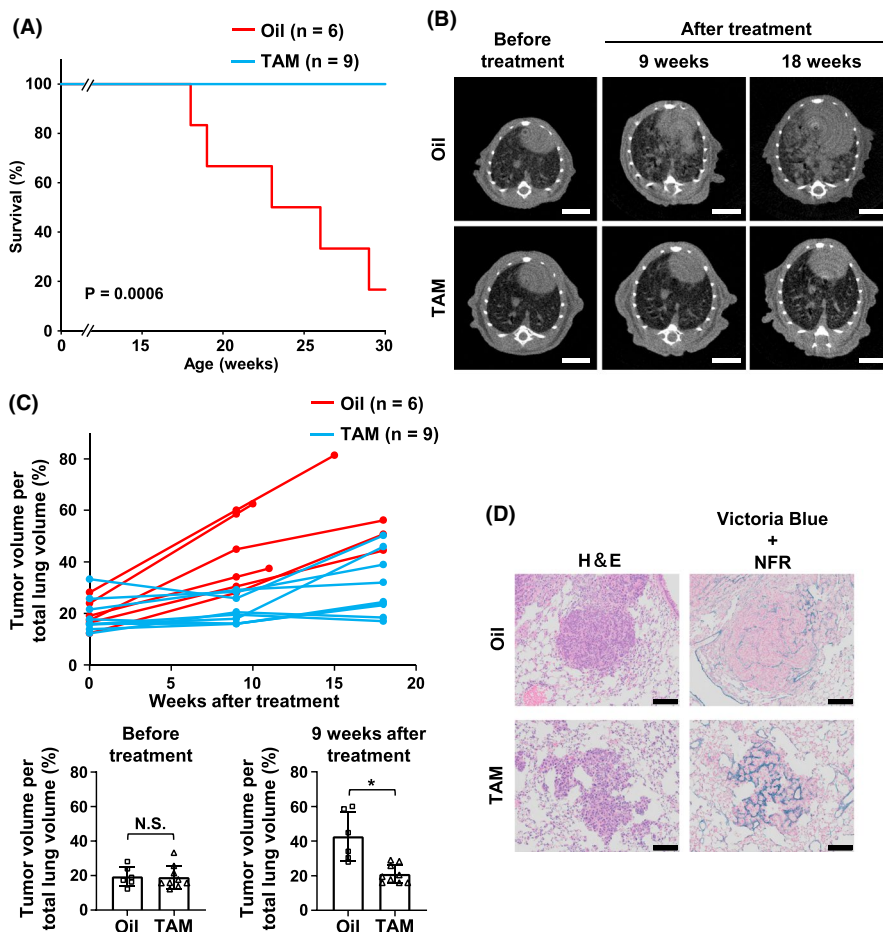


FIGURE 2 *Ror1* required at early stage of lung tumor development. A, Kaplan-Meier survival curves comparing *Ror1^{fl/fl}; CAG-CreER; SPC-hEGFR^{del746-750}* (RCE) mice administered with tamoxifen (TAM) (n = 9) or oil (n = 6). P-values were calculated using a log-rank test. B, Representative axial images of RCE mice administered with TAM or oil at 0, 9, and 18 weeks after treatment. Scale bars represent 5 mm. C, Tumor volume/lung volume ratios calculated using Image J at 0, 9, and 18 weeks after treatment. In bottom panels, columns indicate average and bars standard deviation. P-values were calculated using a two-tailed Student's t-test. NS, not significant. * $P < .05$. D, Representative H&E staining and Victoria blue staining, and counterstaining with nuclear fast red (NFR) of lung tumors from RCE mice administered with TAM (n = 3) or oil (n = 3). Scale bars represent 200 μ m

(Figure 1E,F), which are findings similar to those previously reported for human lung adenocarcinoma cases with increased *TTF-1* and *ROR1* expression.^{6,18,21-23}

To determine the role of *Ror1* in lung tumorigenesis in vivo in an animal model, RCE mice without any detectable lung tumors seen in a micro-CT examination were administered an intraperitoneal (i.p.) injection of 100 mg/kg of TAM once every 5 days from 8 weeks of age. Ablation of *Ror1* significantly delayed tumor development, allowing all mice to survive until 30 weeks of age, whereas control RCE mice administered with oil alone ($n = 6$) showed marked disease progression and a median survival time of 23 weeks ($P = .0006$, log-rank test; Figure 2A-C). Tumors arising in RCE mice conditionally knocked out for *Ror1* with TAM treatment had a considerably preserved existing lung parenchyma architecture as compared with RCE mice treated with the solvent (Figure 2D). Survival curves derived from RE mice treated with TAM ($n = 5$) were not significantly different from those of RCE mice treated with oil alone (Figure S5), indicating that TAM administration did not have a significant effect on survival.

We also examined whether *Ror1* knockout inhibits growth of already detectable tumors because ablation of *Ror1* at an early time point without a detectable tumor may not reflect the therapeutic impact of ROR1 inhibition in future clinical applications. Weekly micro-CT examinations of RCE mice ($n = 9$) from 11 to 16 weeks of age were performed, and i.p. injections of 100 mg/kg of TAM or solvent oil alone once every 5 days were initiated when a tumor larger than 3 mm^2 was detected. *Ror1* ablation resulted in marked retardation of tumor progression, with these RCE mice showing significantly better survival as compared with those treated with the solvent alone ($P = .0031$, log-rank test; Figure 3A-C).

We previously observed that ROR1 knockdown affected RTK signaling towards AKT and p38 in TTF-1/NKX2-1-positive human lung adenocarcinoma cell lines in vitro. However, it was interesting that no readily noticeable changes in regard to activation of Akt, p38 Mapk, Erk, or tyrosine kinase receptors, including EGFR, Met, Her2, and IGF-1R, were observed in tumors arising in RCE mice conditionally knocked out for *Ror1* in the present study (Figure 4A). In this regard, the human mutant *EGFR* transgene was found to be expressed at a very high level (Figure S6), which possibly results in maintaining the activities of these signaling pathways through heterodimerization and transactivation of RTKs,²⁴⁻²⁸ thus conferring insensitivity to

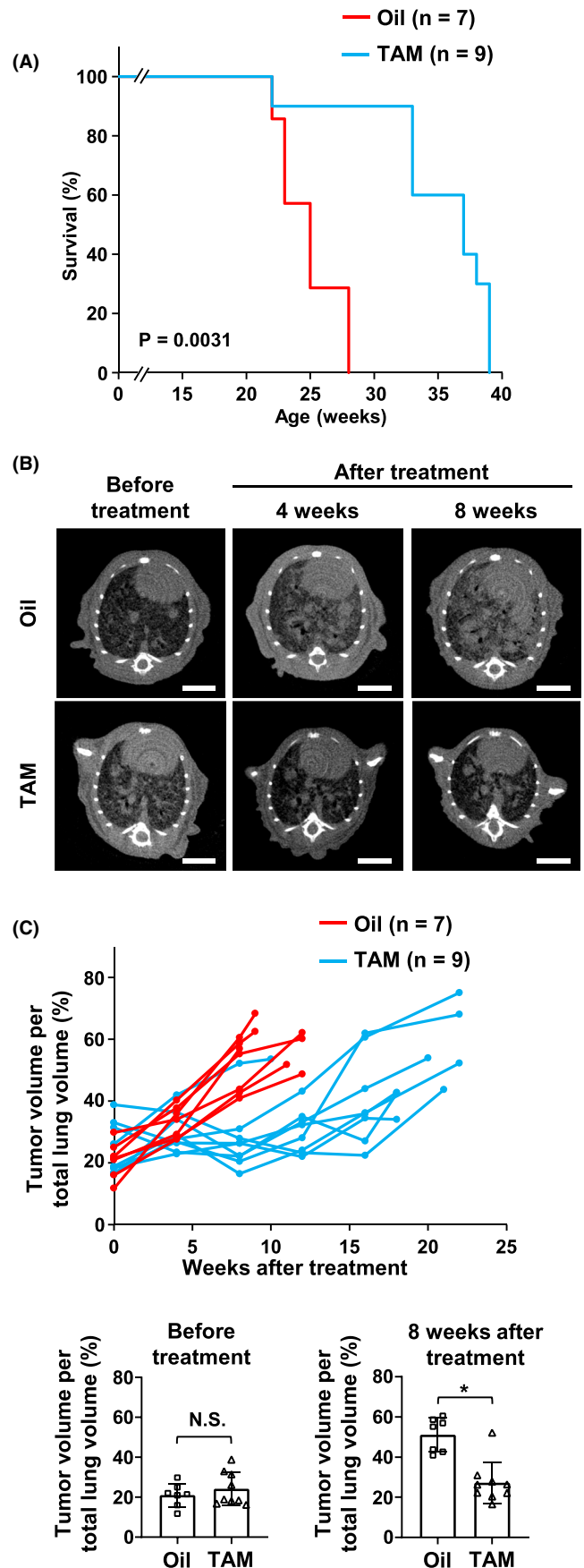


FIGURE 3 *Ror1* ablation delays lung tumor growth. A, Kaplan-Meier survival curves comparing *Ror1*^{fl/fl}; *CAG-CreER*; *SPC-hEGFR*^{del746-750} (RCE) mice administered with tamoxifen (TAM) ($n = 9$) or oil ($n = 7$). P -values were calculated using a log-rank test. B, Representative axial images of RCE mice administered with TAM or oil at 0, 4, and 8 weeks after treatment. Scale bars represent 5 mm. C, Tumor volume/total lung volume ratios were calculated using Image J every 4 weeks after treatment. In bottom panels, columns indicate average and bars standard deviation. P -values were calculated using a two-tailed Student's t -test. NS, not significant. * $P < .05$

Ror1 ablation. Nevertheless, *Ror1* ablation significantly suppressed tumor growth, which was accompanied by a marked decrease in expression of the proliferation marker MCM2 (Figure 4B). We speculated that *Ror1* may also regulate other crucial molecules in lung adenocarcinoma cells. To gain molecular insight into pathways perturbed by *Ror1* knockout in mice, GSEA based on the mRNA expression profiles of lung tumors arising in RCE mice with and without TAM administration was performed. As a result, a gene set of hypoxia-induced genes (HALLMARK_HYPOXIA) was found to be the most significantly downregulated by *Ror1* ablation ($P < .0001$, permutation test; NES = -1.82; FDR = 0.0083; Figure 4C), suggesting a potential regulatory role of *Ror1* in regard to expression of hypoxia-induced genes.

Hypoxia is a commonly observed phenomenon in solid tumors because of an associated rapid increase in tumor mass and disproportional and inadequate tumor angiogenesis.²⁹ Under a hypoxic condition, hypoxia-inducible factor 1 alpha (HIF-1 α) has a pivotal role

to mediate adaptive cellular responses to hypoxia.³⁰ Accordingly, we examined the expression of Hif-1 α in lung tumors that developed in RCE mice. Expression levels of Hif-1 α were greater in lung tumors as compared with normal lung tissues and significantly decreased by *Ror1* ablation (Figure S7A). Furthermore, the expression levels of Hif-1 α target genes associated with glucose metabolism, including *Hk2*, *Ldha*, and *Aldoa*, were significantly decreased in accordance with *Ror1* ablation-mediated suppression of Hif-1 α . On the other hand, expression levels of Hif-1 α -regulated growth factors, such as *Vegfa* and *Tgfa*, were not affected (Figure S7B), suggesting the possibility of maintenance of *Vegfa* and *Tgfa* expression due to *EGFR* transgene overexpression.^{31,32}

Next, whether ROR1 is involved in regulation of HIF-1 α in human lung adenocarcinoma cell lines was examined. ROR1 knockdown using siRNA diminished HIF-1 α expression under normoxia (21% O₂) and clearly hampered induction of HIF-1 α under hypoxia (1% O₂) in NCI-H1975 (Figure 5A), findings that were substantiated by

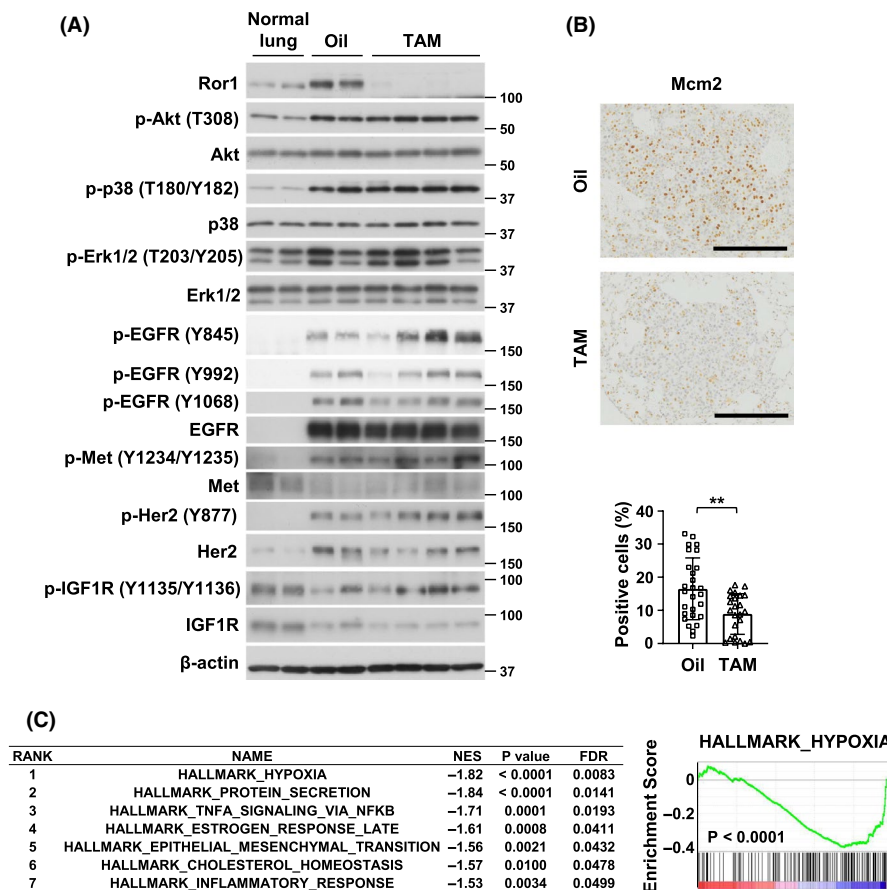


FIGURE 4 Molecular pathways perturbed by *Ror1* ablation in vivo. A, Western blotting analysis of *Ror1*, p-AKT (T308), AKT, p-p38 (T180/Y182), p38, p-Erk1/2 (T203/Y205), Erk1/2, p-EGFR (Y845), p-EGFR (Y992), p-EGFR (Y1068), EGFR, p-Met (Y1234/Y1235), Met, p-Her2 (Y877), Her2, p-IGF1R (Y1135/Y1136), IGF1R, and β -actin in normal lung tissues from *Ror1*^{fl/fl} mice ($n = 2$), and lung tumors from *Ror1*^{fl/fl}; CAG-CreER; SPC-hEGFR^{del746-750} (RCE) mice administered with tamoxifen (TAM) ($n = 4$) or oil ($n = 2$). B, Representative images showing immunohistochemical analysis of MCM2 and percentages of MCM2-positive cells in 24 tumors from RCE mice administered with TAM ($n = 3$) and 27 tumors from RCE mice administered with oil ($n = 3$). Scale bars represent 200 μ m. Columns indicate average and bars standard deviation. ** $P < .01$, two-tailed Student's *t*-test. C, Hallmark gene sets were significantly decreased in lung tumors in RCE mice administered with TAM as compared to those in RCE mice administered oil alone. $P < .01$ and false discovery rate (FDR) $q < 0.05$ were considered to indicate significance. Result for the "HALLMARK_HYPOXIA" gene set was shown on the right. *P*-values were calculated based on gene permutation. NES, normalized enrichment score

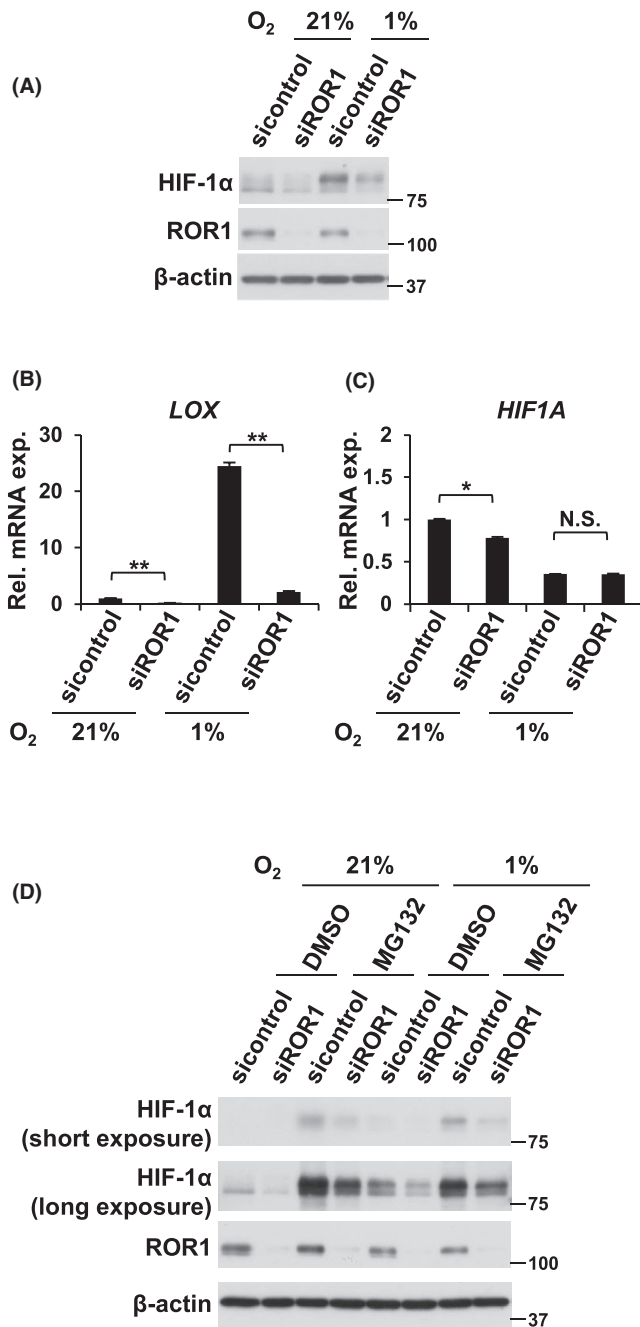


FIGURE 5 Involvement of ROR1 in regulation of HIF-1α protein expression. A, Western blot analysis of ROR1 and HIF-1α under normoxia (21% O₂) or hypoxia (1% O₂). B and C, Quantitative RT-PCR of *LOX* (B) and *HIF1A* (C) in NCI-H1975 cells treated with sicontrol or siROR1 under normoxia (21% O₂) or hypoxia (1% O₂). *P*-values were calculated using a two-tailed Student's *t*-test. NS, not significant. ***P* < .01. D, Western blot analysis of ROR1 and HIF-1α in NCI-H1975 cells treated with sicontrol or siROR1 under normoxia (21% O₂) or hypoxia (1% O₂), with 5 μmol/L MG132 or DMSO for 6 h prior to harvesting. β-actin served as a loading control in experiments shown in (A) and (D)

decreased expression of the hypoxia-responsive, HIF-1α-regulated gene *LOX*²⁹ (Figure 5B). While ROR1 knockdown modestly affected expression levels of *HIF1A* mRNA under normoxia, it did not elicit any changes under hypoxia (Figure 5C). HIF-1α is known to be primarily

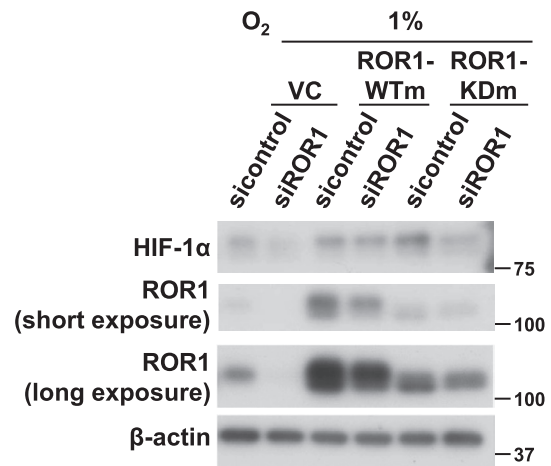


FIGURE 6 Regulation of HIF-1α expression by ROR1 in kinase-dependent manner. Western blot analysis of ROR1 and HIF-1α in presence or absence of siROR1 treatment in NCI-H1975 cells overexpressing siRNA-resistant wild-type (ROR1-WTm) or kinase-dead (ROR1-KDm) ROR1. ROR1-WTm and ROR1-KDm carry multiple silent mutations at the binding site of siROR1.⁶ VC, vector control

controlled by polyubiquitination and proteasomal degradation under normoxia.³³ In this regard, treatment with MG132, a proteasome inhibitor, did not restore HIF-1α protein expression under either a normoxic or hypoxic condition in cells treated with siROR1 (Figure 5D), suggesting involvement of another mechanism in ROR1-mediated regulation of HIF-1α protein. Similar findings were obtained with PC-9 cells (Figure S8A-D). Finally, findings obtained with siROR1-treated NCI-H1975 cells reconstituted with wild-type or kinase-dead ROR1⁶ showed that wild-type but not kinase-dead ROR1 with silent mutations at the siRNA binding site recovered hypoxia-mediated induction of HIF-1α (Figure 6), suggesting that ROR1 regulates HIF-1α expression in a kinase-dependent manner.

4 | DISCUSSION

We and others have previously identified TTF-1/NKX2-1 as a lineage-survival oncogene of lung adenocarcinoma,^{13-16,18} after which our subsequent identification of ROR1 as a crucial downstream factor of TTF-1/NKX2-1-mediated signaling strongly supported the notion of ROR1 as an attractive molecular target for developing novel therapeutics for lung cancers,⁶⁻⁹ as TTF-1/NKX2-1 cannot be targeted due to its essential role in maintaining physiological functions of the lung.^{17,18} In addition, accumulated evidence suggests crucial functions of ROR1 in regulation of cell proliferation, apoptosis, self-renewal of cancer stem cells, epithelial-mesenchymal transition, and metastasis in multiple types of cancer,^{10,34-36} while a significant association of ROR1 expression with worse overall survival has also been reported.^{37,38} These findings have led to exploration of ROR1-targeted therapies, including monoclonal antibodies,^{39,40} CAR-T cells,^{41,42} and small molecule inhibitors.^{43,44} However, to the best of

our knowledge, the importance of *Ror1* in development and progression of any cancer type has never been proven in vivo in an animal model. In the present study, examinations of conditional *Ror1* knockout mice carrying the human mutant *EGFR* transgene demonstrated that conditional *Ror1* ablation strongly inhibits lung tumor development and growth in association with markedly better survival. Interestingly, the lung parenchymal architecture was found to be better preserved in tumor tissues arising in TAM-treated RCE mice as compared with those treated with oil alone, a finding consistent with lower level of malignancy of tumors lacking *Ror1*.

The present results revealed that ROR1 is involved in regulation of HIF-1 α expression in lung adenocarcinoma cells under both normoxic and hypoxic conditions. HIF-1 α is a master regulator of adaptive responses to hypoxia and has profound effects on various aspects of cancer development, including proliferation, angiogenesis, metabolism, migration and invasion, metastasis, resistance to therapy, and poor prognosis.^{29,30,33,45} Therefore, direct targeting of HIF-1 α or inhibition of downstream effector pathways is considered to have great promise for treatment of cancer. In addition, targeting RTKs has been suggested as an alternative means to suppress HIF-1 α -mediated signaling.⁴⁶⁻⁴⁹ In this regard, HER2 and EGFR have been shown to induce HIF-1 α protein via the PI3K/AKT/MTOR signaling pathway in breast cancer cell lines,^{46,47} while VEGF/VEGFR1-mediated MAPK signaling was found to promote HIF-1 α transcriptional activity in neuroblastoma cells by increasing phosphorylation of HIF-1 α .⁴⁸ It was also reported that various RTKs, including VEGFR1, PDGFR- β , RET, and EGFR, regulate HIF-1 α mRNA expression.⁴⁹ Notably, inhibition of a single RTK was shown to have only a minimal effect on HIF-1 α expression, perhaps because of redundant regulation of HIF-1 α by multiple RTKs. With this in mind, it is interesting to note that the present results clearly demonstrated that ROR1 inhibition alone was sufficient to suppress HIF-1 α expression under both normoxic and hypoxic conditions despite sustainment of RTK signaling.

In conclusion, conditional *Ror1* knockout mice carrying a human mutant *EGFR* transgene were established in the present study. Experiments with that animal model clearly demonstrated for the first time that *Ror1* has crucial involvement in lung adenocarcinoma development and growth in vivo. In addition, the importance of ROR1 in regulation of HIF-1 α expression was also shown. ROR1 thus appears to be a promising molecular target for the development of a novel therapeutic to treat solid tumors such as lung cancer, which are frequently accompanied with a hypoxic microenvironment.

ACKNOWLEDGMENTS

We would like to thank Jeffrey A. Whitsett at Cincinnati Children's Hospital for the generous gift of a human SP-C promoter construct; Ken-ichi Yamamura and members of the Center for Animal Resources and Development, Kumamoto University, for their contributions to the generation of human mutant *EGFR* transgenic mice; Masahiro Aoki at the Division of Pathophysiology, Aichi Cancer Center Research Institute, for various technical help and arrangements; and Atsushi Enomoto at the Department of Pathology, Nagoya University Graduate School of

Medicine, for the helpful discussion. This work was supported in part by a Grant-in-Aid for Scientific Research (A; 16H02468) from the Japan Society for the Promotion of Science, as well as grants from the Project for Development of Innovative Research on Cancer Therapeutics (P-Direct, JP18cm0106107) and Project for Cancer Research and Therapeutic Evolution (P-CREATE, JP20cm0106107) from the Japan Agency for Medical Research and Development (AMED).

DISCLOSURE

The authors have no competing interests to declare.

ORCID

Masahiro Nakatochi  <https://orcid.org/0000-0002-1838-4837>

Motoshi Suzuki  <https://orcid.org/0000-0003-0682-5006>

Tomoya Yamaguchi  <https://orcid.org/0000-0001-6933-543X>

Takashi Takahashi  <https://orcid.org/0000-0003-0615-7001>

REFERENCES

- Green JL, Kuntz SG, Sternberg PW Ror receptor tyrosine kinases: orphans no more. *Trends Cell Biol.* 2008;18:536-544.
- Nomi M, Oishi I, Kani S, et al. Loss of mRor1 enhances the heart and skeletal abnormalities in mRor2-deficient mice: redundant and pleiotropic functions of mRor1 and mRor2 receptor tyrosine kinases. *Mol Cell Biol.* 2001;21:8329-8335.
- Ho HY, Susman MW, Bikoff JB, et al. Wnt5a-Ror-Dishevelled signaling constitutes a core developmental pathway that controls tissue morphogenesis. *Proc Natl Acad Sci USA.* 2012;109:4044-4051.
- Fukuda T, Chen L, Endo T, et al. Antisera induced by infusions of autologous Ad-CD154-leukemia B cells identify ROR1 as an oncofetal antigen and receptor for Wnt5a. *Proc Natl Acad Sci USA.* 2008;105:3047-3052.
- Zhang S, Chen L, Wang-Rodriguez J, et al. The onco-embryonic antigen ROR1 is expressed by a variety of human cancers. *Am J Pathol.* 2012;181:1903-1910.
- Yamaguchi T, Yanagisawa K, Sugiyama R, et al. NKX2-1/TITF1/TTF-1-Induced ROR1 is required to sustain EGFR survival signaling in lung adenocarcinoma. *Cancer Cell.* 2012;21:348-361.
- Yamaguchi T, Lu C, Ida L, et al. ROR1 sustains caveolae and survival signalling as a scaffold of cavin-1 and caveolin-1. *Nat Commun.* 2016;7:10060.
- Yamaguchi T, Hayashi M, Ida L, et al. ROR1-CAVIN3 interaction required for caveolae-dependent endocytosis and pro-survival signaling in lung adenocarcinoma. *Oncogene.* 2019;38:5142-5157.
- Ida L, Yamaguchi T, Yanagisawa K, et al. Receptor tyrosine kinase-like orphan receptor 1, a target of NKX2-1/TTF-1 lineage-survival oncogene, inhibits apoptosis signal-regulating kinase 1-mediated pro-apoptotic signaling in lung adenocarcinoma. *Cancer Sci.* 2016;107:155-161.
- Bicocca VT, Chang BH, Masouleh BK, et al. Crosstalk between ROR1 and the Pre-B cell receptor promotes survival of t(1;19) acute lymphoblastic leukemia. *Cancer Cell.* 2012;22:656-667.
- Daneshmanesh AH, Porwit A, Hojjat-Farsangi M, et al. Orphan receptor tyrosine kinases ROR1 and ROR2 in hematological malignancies. *Leuk Lymphoma.* 2013;54:843-850.
- Balakrishnan A, Goodpaster T, Randolph-Habecker J, et al. Analysis of ROR1 protein expression in human cancer and normal tissues. *Clin Cancer Res.* 2017;23:3061-3071.
- Tanaka H, Yanagisawa K, Shinjo K, et al. Lineage-specific dependency of lung adenocarcinomas on the lung development regulator TTF-1. *Cancer Res.* 2007;67:6007-6011.
- Weir BA, Woo MS, Getz G, et al. Characterizing the cancer genome in lung adenocarcinoma. *Nature.* 2007;450:893-898.

15. Kendall J, Liu Q, Bakleh A, et al. Oncogenic cooperation and co-amplification of developmental transcription factor genes in lung cancer. *Proc Natl Acad Sci USA*. 2007;104:16663-16668.
16. Kwei KA, Kim YH, Girard L, et al. Genomic profiling identifies TTF1 as a lineage-specific oncogene amplified in lung cancer. *Oncogene*. 2008;27:3635-3640.
17. Maeda Y, Dave V, Whitsett JA Transcriptional control of lung morphogenesis. *Physiol Rev*. 2007;87:219-244.
18. Yamaguchi T, Hosono Y, Yanagisawa K, Takahashi T NKX2-1/TTF-1: an enigmatic oncogene that functions as a double-edged sword for cancer cell survival and progression. *Cancer Cell*. 2013;23:718-723.
19. Griesing S, Kajino T, Tai MC, et al. Thyroid transcription factor-1-regulated microRNA-532-5p targets KRAS and MKL2 oncogenes and induces apoptosis in lung adenocarcinoma cells. *Cancer Sci*. 2017;108:1394-1404.
20. Subramanian A, Tamayo P, Mootha VK, et al. Gene set enrichment analysis: a knowledge-based approach for interpreting genome-wide expression profiles. *Proc Natl Acad Sci USA*. 2005;102:15545-15550.
21. Yatabe Y, Kosaka T, Takahashi T, Mitsudomi T EGFR mutation is specific for terminal respiratory unit type adenocarcinoma. *Am J Surg Pathol*. 2005;29:633-639.
22. Takeuchi T, Tomida S, Yatabe Y, et al. Expression profile-defined classification of lung adenocarcinoma shows close relationship with underlying major genetic changes and clinicopathologic behaviors. *J Clin Oncol*. 2006;24:1679-1688.
23. Yatabe Y, Mitsudomi T, Takahashi T TTF-1 expression in pulmonary adenocarcinomas. *Am J Surg Pathol*. 2002;26:767-773.
24. Lemmon MA, Schlessinger J, Ferguson KM The EGFR family: not so prototypical receptor tyrosine kinases. *Cold Spring Harb Perspect Biol*. 2014;6:a020768.
25. Dong Q, Du Y, Li H, et al. EGFR and c-MET cooperate to enhance resistance to PARP inhibitors in hepatocellular carcinoma. *Cancer Res*. 2019;79:819-829.
26. Tanizaki J, Okamoto I, Sakai K, Nakagawa K Differential roles of trans-phosphorylated EGFR, HER2, HER3, and RET as heterodimerisation partners of MET in lung cancer with MET amplification. *Br J Cancer*. 2011;105:807-813.
27. Nahta R, Yuan LX, Zhang B, Kobayashi R, Esteva FJ Insulin-like growth factor-I receptor/human epidermal growth factor receptor 2 heterodimerization contributes to trastuzumab resistance of breast cancer cells. *Cancer Res*. 2005;65:11118-11128.
28. Barnes CJ, Ohshiro K, Rayala SK, El-Naggar AK, Kumar R Insulin-like growth factor receptor as a therapeutic target in head and neck cancer. *Clin Cancer Res*. 2007;13:4291-4299.
29. Bertout JA, Patel SA, Simon MC The impact of O₂ availability on human cancer. *Nat Rev Cancer*. 2008;8:967-975.
30. Semenza GL Hypoxia-inducible factors in physiology and medicine. *Cell*. 2012;148:399-408.
31. Lichtenberger BM, Tan PK, Niederleithner H, Ferrara N, Petzelbauer P, Sibilica M Autocrine VEGF signaling synergizes with EGFR in tumor cells to promote epithelial cancer development. *Cell*. 2010;140:268-279.
32. Zhao Y, Kaushik N, Kang JH, et al. A feedback loop comprising EGF/TGF α sustains TFCP2-mediated breast cancer progression. *Cancer Res*. 2020;80:2217-2229.
33. Kaelin WG Jr, Ratcliffe PJ Oxygen sensing by metazoans: the central role of the HIF hydroxylase pathway. *Mol Cell*. 2008;30:393-402.
34. Zhang S, Cui B, Lai H, et al. Ovarian cancer stem cells express ROR1, which can be targeted for anti-cancer-stem-cell therapy. *Proc Natl Acad Sci USA*. 2014;111:17266-17271.
35. Li C, Wang S, Xing Z, et al. A ROR1-HER3-lncRNA signalling axis modulates the Hippo-YAP pathway to regulate bone metastasis. *Nat Cell Biol*. 2017;19:106-119.
36. Cui B, Zhang S, Chen L, et al. Targeting ROR1 inhibits epithelial-mesenchymal transition and metastasis. *Cancer Res*. 2013;73:3649-3660.
37. Anagnostou VK, Syrigos KN, Bepler G, Homer RJ, Rimm DL Thyroid transcription factor 1 is an independent prognostic factor for patients with stage I lung adenocarcinoma. *J Clin Oncol*. 2009;27:271-278.
38. Saleh RR, Antras JF, Peinado P, et al. Prognostic value of receptor tyrosine kinase-like orphan receptor (ROR) family in cancer: a meta-analysis. *Cancer Treat Rev*. 2019;77:11-19.
39. Choi MY, Widhopf GF, Ghia EM, et al. Phase I trial: cirmtuzumab inhibits ROR1 signaling and stemness signatures in patients with chronic lymphocytic leukemia. *Cell Stem Cell*. 2018;22(951-9):e3.
40. Choi MY, Widhopf GF, Wu CCN, et al. Pre-clinical specificity and safety of UC-961, a first-in-class monoclonal antibody targeting ROR1. *Clin Lymphoma Myeloma Leuk*. 2015;15(Suppl):S167-S169.
41. Hudecek M, Lupo-Stanghellini MT, Kosasih PL, et al. Receptor affinity and extracellular domain modifications affect tumor recognition by ROR1-specific chimeric antigen receptor T cells. *Clin Cancer Res*. 2013;19:3153-3164.
42. Srivastava S, Salter AI, Liggitt D, et al. Logic-gated ROR1 chimeric antigen receptor expression rescues T cell-mediated toxicity to normal tissues and enables selective tumor targeting. *Cancer Cell*. 2019;35(489-503):e8.
43. Hojjat-Farsangi M, Daneshmanesh AH, Khan AS, et al. First-in-class oral small molecule inhibitor of the tyrosine kinase ROR1 (KAN0439834) induced significant apoptosis of chronic lymphocytic leukemia cells. *Leukemia*. 2018;32:2291-2295.
44. Ghaderi A, Daneshmanesh AH, Moshfegh A, et al. ROR1 is expressed in diffuse large B-cell lymphoma (DLBCL) and a small molecule inhibitor of ROR1 (KAN0441571C) induced apoptosis of lymphoma cells. *Biomedicines*. 2020;8:170.
45. LaGory EL, Giaccia AJ The ever-expanding role of HIF in tumour and stromal biology. *Nat Cell Biol*. 2016;18:356-365.
46. Laughner E, Taghavi P, Chiles K, Mahon PC, Semenza GL HER2 (neu) signaling increases the rate of hypoxia-inducible factor 1 α (HIF-1 α) synthesis: novel mechanism for HIF-1-mediated vascular endothelial growth factor expression. *Mol Cell Biol*. 2001;21:3995-4004.
47. Peng XH, Karna P, Cao Z, Jiang BH, Zhou M, Yang L Cross-talk between epidermal growth factor receptor and hypoxia-inducible factor-1 α signal pathways increases resistance to apoptosis by up-regulating survivin gene expression. *J Biol Chem*. 2006;281:25903-25914.
48. Das B, Yeger H, Tsuchida R, et al. A hypoxia-driven vascular endothelial growth factor/Flt1 autocrine loop interacts with hypoxia-inducible factor-1 α through mitogen-activated protein kinase/extracellular signal-regulated kinase 1/2 pathway in neuroblastoma. *Cancer Res*. 2005;65:7267-7275.
49. Nilsson MB, Zage PE, Zeng L, et al. Multiple receptor tyrosine kinases regulate HIF-1 α and HIF-2 α in normoxia and hypoxia in neuroblastoma: implications for antiangiogenic mechanisms of multikinase inhibitors. *Oncogene*. 2010;29:2938-2949.

SUPPORTING INFORMATION

Additional supporting information may be found online in the Supporting Information section.

How to cite this article: Isomura H, Taguchi A, Kajino T, et al. Conditional *Ror1* knockout reveals crucial involvement in lung adenocarcinoma development and identifies novel HIF-1 α regulator. *Cancer Sci*. 2021;112:1614-1623. <https://doi.org/10.1111/cas.14825>